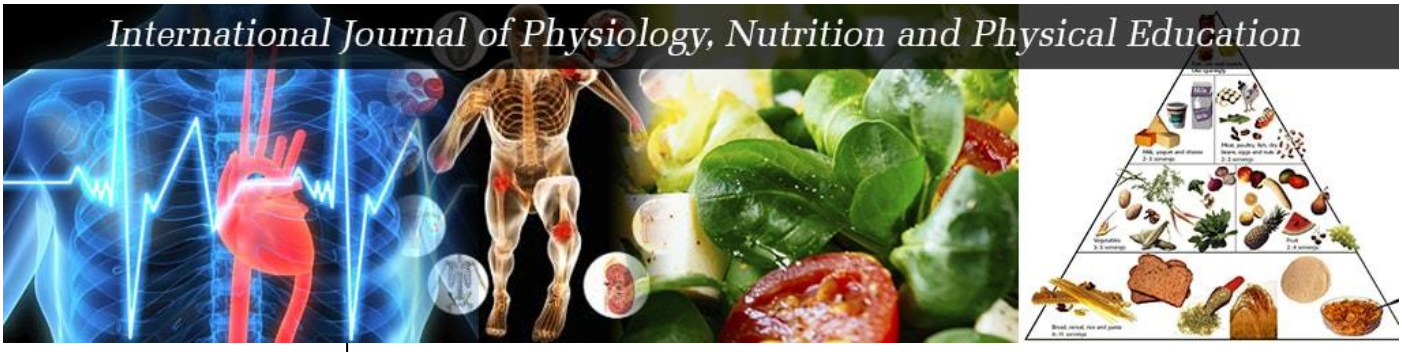

ISSN: 2456-0057
IJPNPE 2020; 5(1): 100-108
© 2020 IJPNPE
www.journalofsports.com
Received: 08-11-2019
Accepted: 12-12-2019

Abhijit Maiti
Assistant Professor, Physiology Department, Rajiv Gandhi Medical College, Kalwa, Thane, Maharashtra, India

Poorva Bhave
Assistant Professor, Microbiology Department, Rajiv Gandhi Medical College, Kalwa, Thane, Maharashtra, India

Kakuli Maiti
Assistant Professor, Humanities and Sciences Department, Datta Meghe College of Engineering, Sector-3, Airoli, Navi Mumbai, Maharashtra, India

Corresponding Author:
Abhijit Maiti
Assistant Professor, Physiology Department, Rajiv Gandhi Medical College, Kalwa, Thane, Maharashtra, India

Zinc oxide nanoparticles as alternatives for overcoming antibiotic resistance in food-borne pathogenic bacteria

Abhijit Maiti, Poorva Bhave and Kakuli Maiti

Abstract
Zinc oxide nanoparticles and zinc oxide nanoparticles doped with vanadium and nickel were synthesised by sol-gel method and their structural, morphological and antibacterial activity were studied. X-Ray Diffraction studies revealed that all synthesised materials were crystalline and vanadium and nickel had created defect sites resulting into planes by the presence of extra peaks in the doped samples. The surface morphology of zinc oxide nanoparticles was significantly modified by doping with vanadium and nickel. The absorption edge of zinc oxide had red-shifted with increase in doping concentration of transition metal vanadium and nickel. The antibacterial activity of the particles was quantified with MIC and MBC and thus bactericidal dosage using one Gram-positive and one Gram-negative bacteria. Food borne pathogens can be controlled by these nanoparticles and thus food packaging industry may get some enhancement in their armoury of anti-bacterial agents against food borne diseases.

Keywords: Antibacterial activity, nanoparticles, photocatalysis, zinc oxide

1. Introduction
ZnO is a versatile functional, promising inorganic material. It is having a unique optical, chemical sensing, semiconducting, electric conductivity and piezo electric properties in the nanometre range [1]. ZnO is a direct band gap (3.3 eV) semi-conductor with near UV absorption (UVA 315-400 nm and UVB 280-315 nm) region in spectrum, a high excitonic binding energy (60 meV) at room temperature and a natural n-type electrical conductivity [2-8]. The wide band gap of ZnO has a significant effect on its properties such as the electrical, conductivity and optical absorption. The excitonic emission and the electrical conductivity increases when ZnO is doped with other metals [2]. ZnO has properties, such as, durability, higher selectivity and heat resistance, with proven anti-bacterial, anti-fungal agent and is used as a UV protector in cosmetics and food industries [8] and is a preferred inorganic material [9].
The ZnO nanoparticles (ZnO NPs) can interact with bacterial surface and/or with bacterial core where it enters inside the cell [10]. It is being reported in several studies that ZnO NPs are non-toxic to human cells [11] with good bio-compatibility to human cells and their usage as anti-bacterial agent noxious to microorganism holds a vast field of study [12]. Increase in bacterial antibiotic resistance, emergence of new bacterial mutation is a challenging problem as a global health hazard. Thus developing novel anti-bacterial agents against bacterial strains found as food pathogen such as *Escherichia coli* and *Staphylococcus aureus*.
ZnO has intrinsic defects, such as, oxygen vacancies (V_o), zinc vacancies (V_{Zn}) and zinc interstials (Zn_i) making it a suitable material by doping with selected material for various applications. The transition metal doping in semi-conductor facilitates the generation of carrier-mediated ferromagnetism [13]. Nickel is considered to be the most capable transition metal dopant due to its high chemical stability and exceptional ability to tune electrical, optical and magnetic behaviour of ZnO nano structure [14].
ZnO doped with vanadium showed improved optical properties [15] due to increased carrier lifetime, V-doped ZnO are used in optical devices like lasers, optical detectors, transparent conductive oxide, solar cells, and spintronic material and photo electro chemistry [16]. ZnO is used to treat variety of skin conditions in products, such as, baby powder and barrier creams (to treat diaper rash), calamine cream, anti-dandruff shampoos and anti-septic ointments [17]. It is also a component in tape ("ZnO tape") used by athletes as a bandage to prevent soft tissue

damage during workouts [18]. When used as an ingredient in sunscreen lotion, ZnO sits on the skin's surface and is not absorbed into the skin, which blocks UVA and UVB rays of ultraviolet light. It is approved for use as a sunscreen by the Food and Drug Administration (FDA).

This work focuses on the synthesis of ZnO-Ni and ZnO-V by sol-gel technique and studies the effect of doping on the structural and morphological properties. ZnO NPs are known to be one of the multifunctional inorganic nanoparticles with effective antibacterial activity. In this study, we considered antibacterial activity of Ni and V doped ZnO NPs.

2. Materials and Methods

2.1 Material

Zinc Acetate dihydrate, Oxalic acid dihydrate, nickel (ll) nitrate hexahydrate, Ammonium metavandate were purchased from Merck with 98% purity. Ethanol and double distilled water was used as the solvent and all the chemicals were used without further treatment.

2.2 Synthesis

In this study, ZnO NPs were synthesised using the sol-gel method. Zinc Acetate Dihydrate and oxalic acid dihydrate were used as precursors. Ethanol and double distilled water 10% by volume is used as solvent and a molar ratio of 1:2 is found to give efficient product. Nickel Nitrate Hexa hydrate and Ammonium metavandate were used in required amount for 10 at % doping. Steps of washing with ethanol were followed, dried, pestered and annealed for 2 hours at 600ºC.

2.3 Characterisation

All the as prepared samples were characterised using Rigaku Ultima IV X-Ray Diffractometer (Rigaku Corporation, Tokyo, Japan) by CuK_α (λ = 1.5414ºA) radiation, in Bragg-Brentano (θ-2θ) configuration from 20º - 80º in a step of 2º per minute. The surface area of the NPs was calculated using Smart Sorb 93, Brunauer-Emmett-Teller (BET) surface analyser with liquid nitrogen in Dewar cryogenic storage for adsorption calibration. UV-Vis absorption spectra (in DRS mode) was absorbed using Carry 500 UV-Vis-NIR spectrophotometer in the range of 200-800nm. The surface morphology of all the samples was studied by Scanning electron microscope (SEM). JEOL, FEG, JSM 700LF, X-Ray photo electron spectra were acquired using a Phi 5000 Versa Probe II equipped with a monochromatic AlK_α (1486.6 eV) X-Ray source and a hemispherical analyser.

2.4 Antibacterial Culture

In this part of the experiment to measure the minimum inhibitory concentration (MIC) for each organism, a set of seven tubes, one containing 2 ml of double strength Mueller Hinton broth (DS MH Broth) and remaining 6 tubes containing 2 ml of single strength Mueller Hinton broth (SS MH Broth) were arranged in a row. In 50 ml of distilled water, 1.6 gram of ZnO powder was mixed to prepare uniform suspension. This was used as stock solution (1600 µg/ml). Two ml of stock solution was added to first tube (2 ml DS MH broth). The solution was mixed well and 2 ml of it was transferred to the second tube (2 ml SS MH broth). The procedure was repeated till last tube and finally 2 ml was discarded from the last tube. In this way, serial doubling dilutions ranging from 1600 µg / ml to 25 µg / ml were obtained. Standard strains of *Staphylococcus aureus* and *Escherichia coli* were incubated overnight in the nutrient broth. To each of the set of seven tubes, 50 µl of *Staphylococcus aureus* broth matched to McFarland 0.5 standard was added. Similarly in the second set of seven tubes 50µl of *Escherichia coli* broth matched to McFarland 0.5 standard was added. Tubes were incubated at 35°C for 24 h. Result was read as break point value for the minimum concentration at which broth showed turbidity. Minimum bactericidal concentration (MBC) was estimated by sub-culturing from broth tubes that showed no growth on solid media. Similar procedure, repeated for all of the samples, measured the MIC and the MBC, which were tabulated.

3. Results and Discussion

3.1 Characterisation of nanoparticles

The Brunaver-Emmelt-Teller (BET) principle of surface analysis of various prepared samples using the physical adsorption of gas molecules on the solid surface was studied and tabulated (Table-1). All the samples were analysed using standard procedure of instrument with sample weight less than 0.7 gram degassed for 2 hrs at 120ºC.

Table 1: Size, BET surface area, Band gap of the samples.

Sample Name	Size (nm)	Surface Area (m^2/gm)	Band Gap (eV)
ZnO	33.84	12.5	3.20
ZnO-10V	29.61	7.54	2.89
ZnO-10Ni	54.32	6.29	3.18

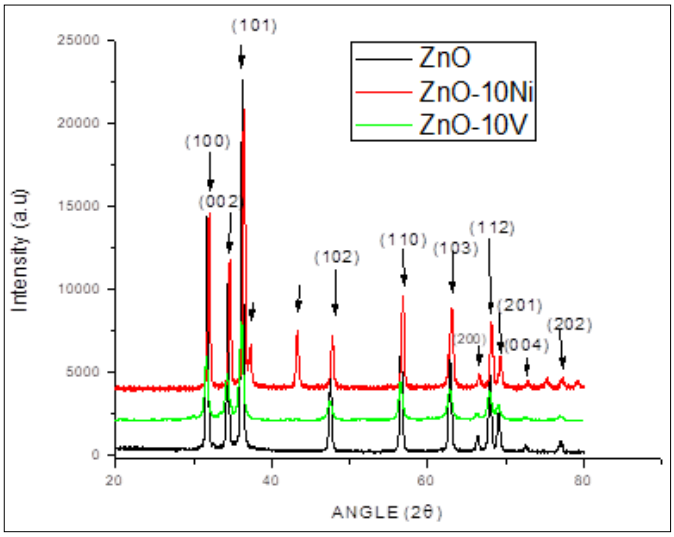

Fig 1: X-ray Diffraction graph of ZnO, ZnO-10V, ZnO-10Ni

The comparative X-ray Diffraction (XRD) graph of ZnO, ZnO-10V, ZnO-10Ni (Figure-1) showed that all the samples are highly crystalline nano Xerogel. ZnO peaked at 31.79°, 34.39°, 36.22°, 47.50°, 56.54°, 62.80°, 66.31°, 67.68°, 69.02°, 72.52°, 76.58°, observed with peak shift towards higher angle with increase in doping concentration of vanadium and nickel. The Miller Index of the planes were (100), (002), (101), (102), (110), (103), (200), (112), (201), (004), (202)

A shoulder peak was observed at 37.29° for ZnO-10Ni at plane (111).Other extra peaks observed were at 43.33°,72.32°, 75.18°, 79.29° having indices (012), (104), (113), (006) showed that Ni and V ions had occupied different position in the hexagonal wurtzite lattice of zinc oxide forming defect planes. (DB card no. 10-080-0075, JCPDS card 37-1485 and others). The particle size, calculated using Debye-Scherer formula with FWHM, was 15nm -65nm. Lattice parameter of ZnO a = b = 3.254A°, c = 5.24A°, FWHM = .297, volume = 47.359, hexagonal unit cell. Space group 186: p63mc, card no

01-080-0075.inter planar spacing was in the range of 1.233-2.989A° with bond length 1.9861 A°.

The absorption spectra measured in diffused reflectance mode of ZnO, ZnO-10V, ZnO-10Ni showed a red shift which increases with increase in doping concentration. The band gap energies were calculated with Kubleka Munk function and Tauc plot (Figures-2 & 3), thus the extrapolating the tail end on the photon energy axis was tabulated (Table-1).

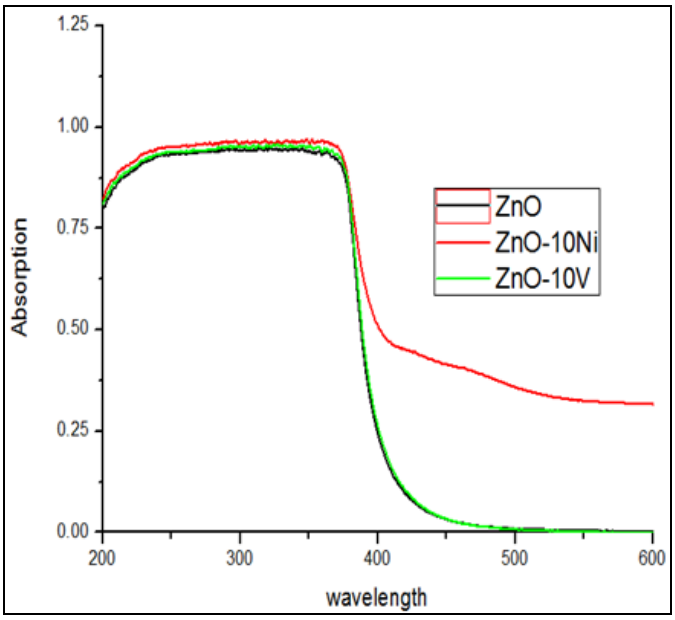

Fig 2: UV absorption of ZnO, ZnO-10v, ZnO-10Ni

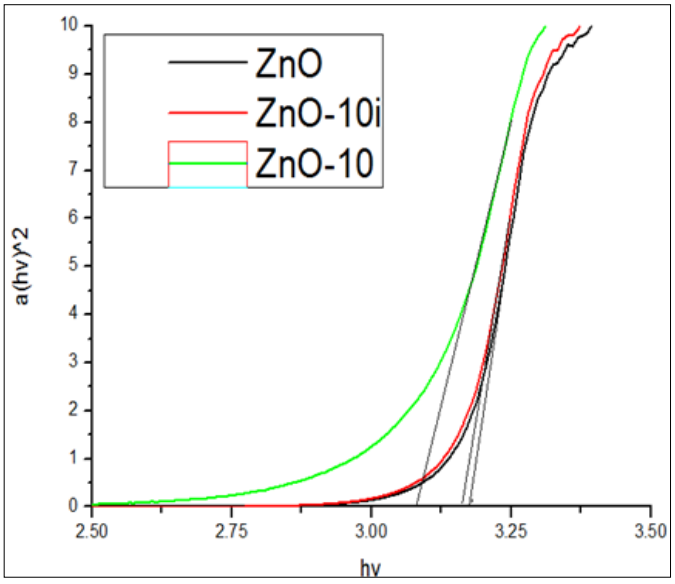

Fig 3: Tauc Plot of ZnO, ZnO-10V ZnO-10Ni

Surface morphology of all the samples was examined using Scanning Electron Microscope or SEM (Figures-4, 5 & 6) and, they were in good agreement with the calculated crystallite size obtained from XRD by Scherrer formula. Most of the particles were spherical; some rod-like structures were also present with increase in doping element**.** The chemical composition and electronic structure of the ZnO and doped ZnO was investigated by X-ray photoelectron spectroscopy (XPS).

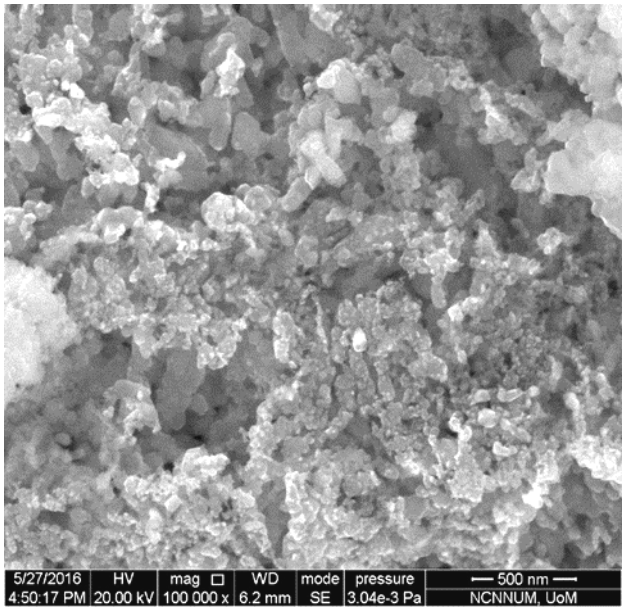

Fig 4: SEM image of ZnO-V, ZnO, ZnO-Ni.

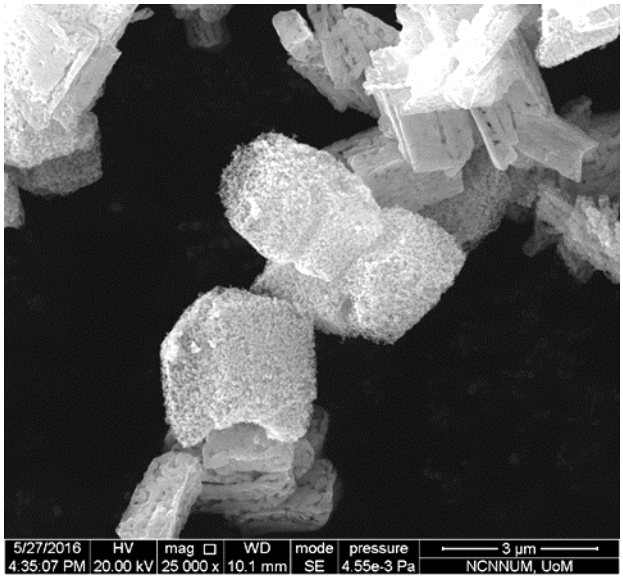

Fig 5: SEM image of ZnO-V, ZnO, ZnO-Ni.

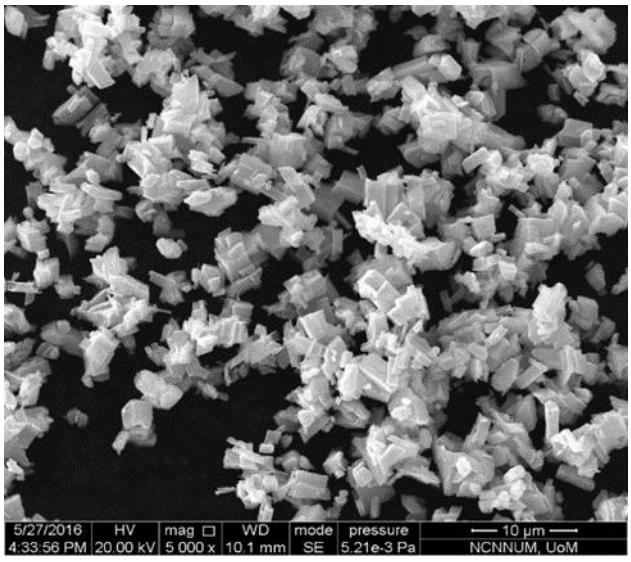

Fig 6: SEM image of ZnO-V, ZnO, ZnO-Ni.

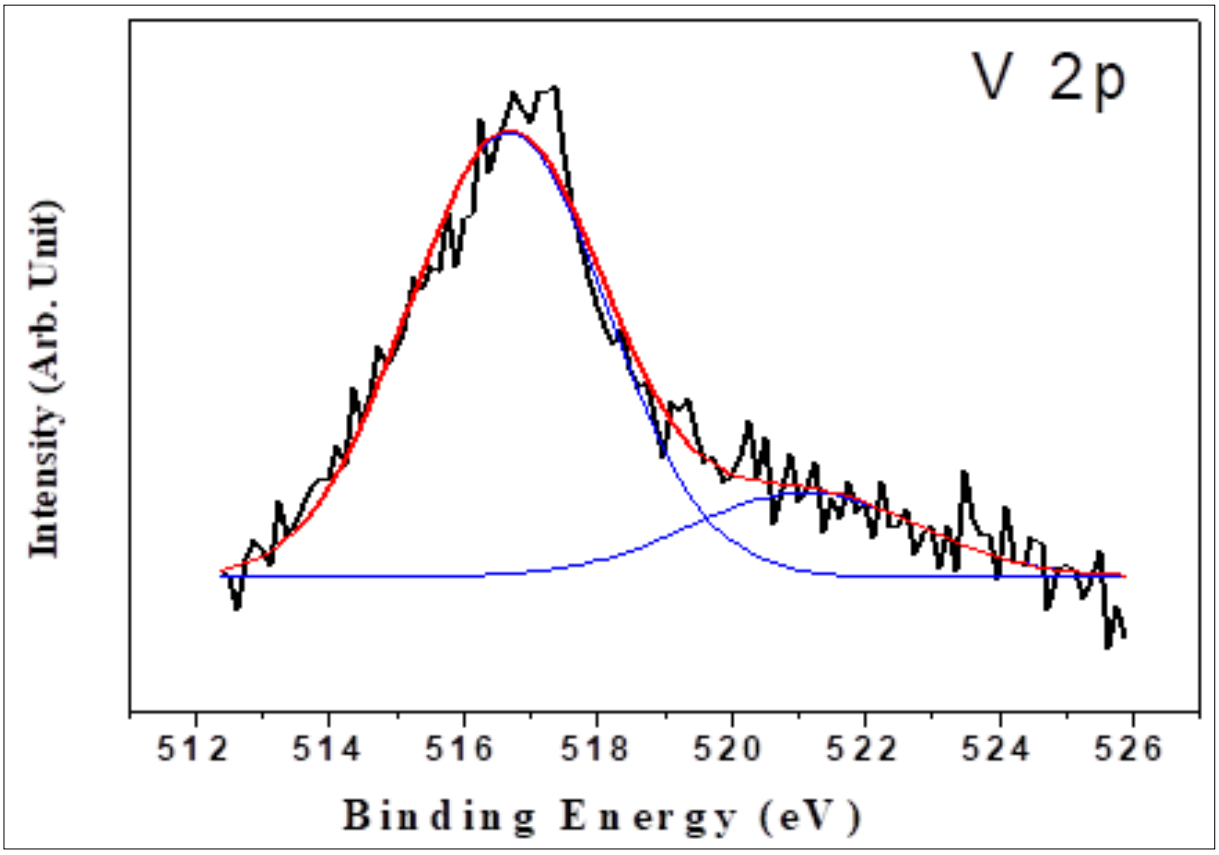

Fig 7: XPS peak of Vanadium

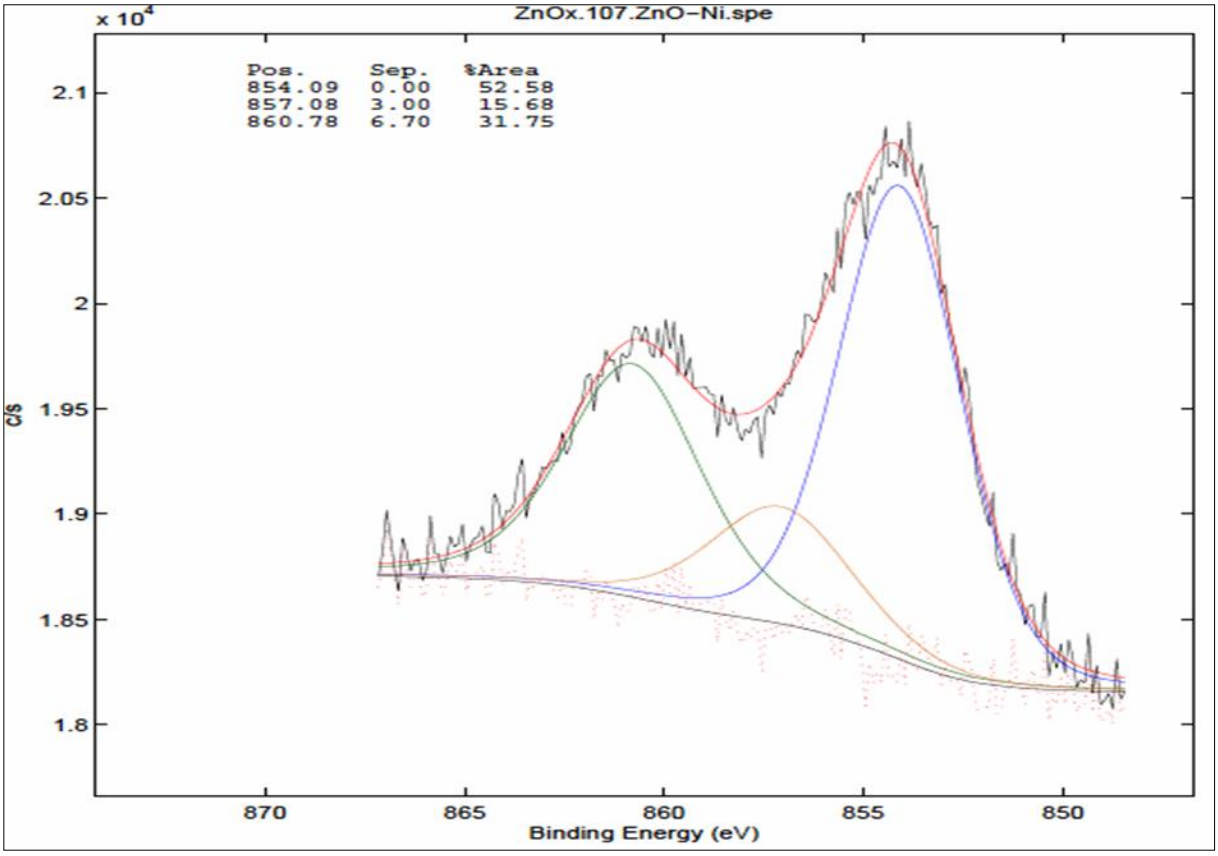

Fig 8: XPS peak of Nickel

The survey and core-shell level X-ray photoelectron spectroscopy (XPS) Spectra of Zn-2p, O-1s as well as valence band of ZnO and doped ZnO-10Ni are shown in figures-7, 8 & 9.

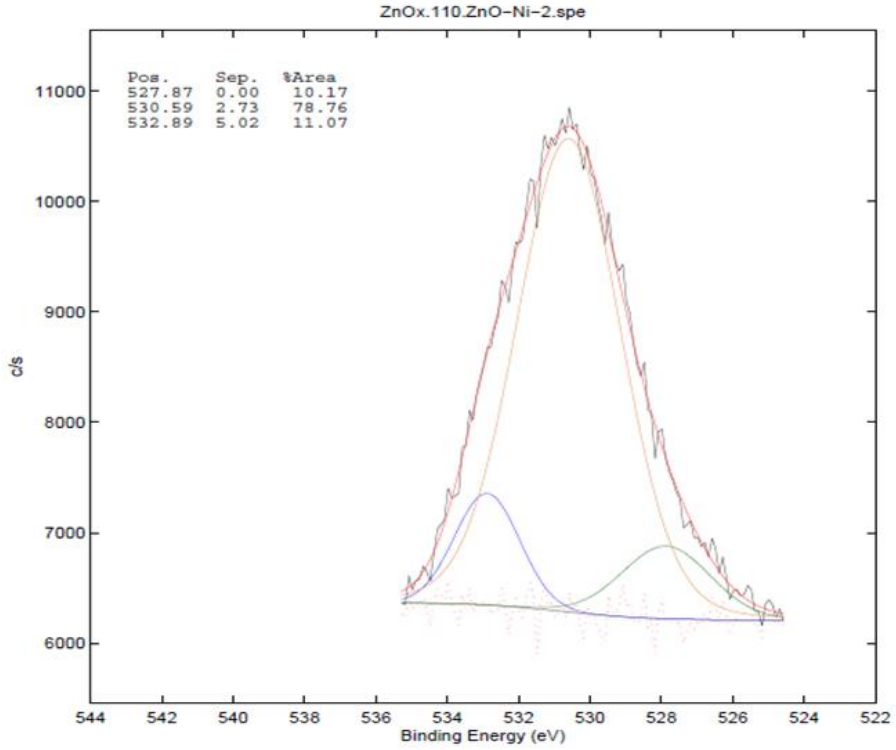

Fig 9: XPS peak of Oxygen.

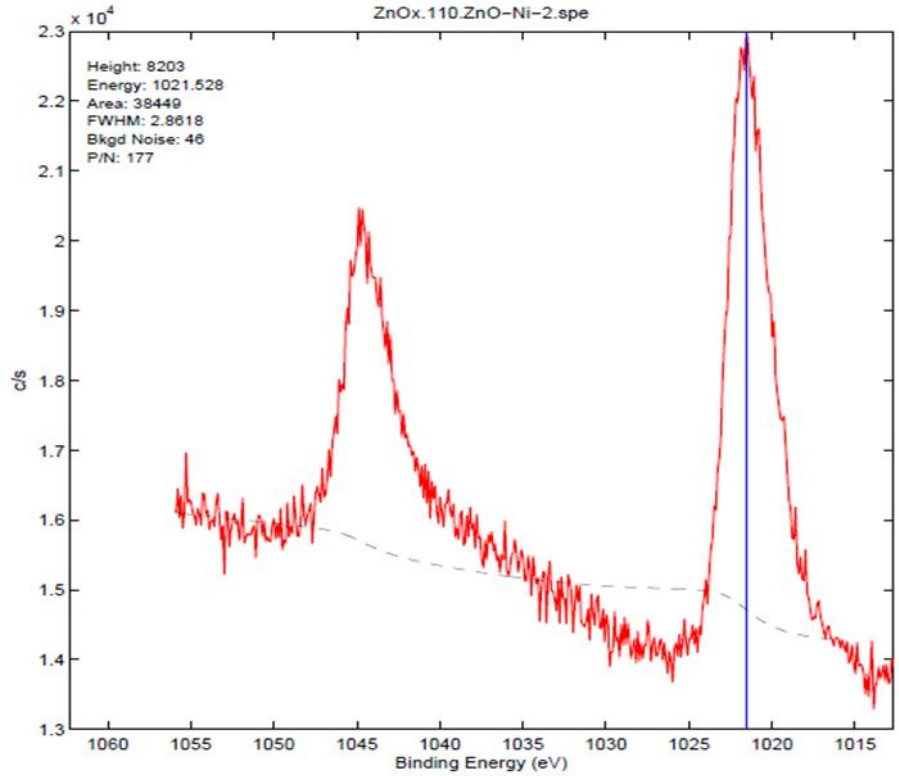

Fig 10: XPS peak of Zn

The characteristics intense peaks were centred at 1021.06 eV (Zn2p3/2) and 1044.70 eV (Zn2p1/2) from Spectra of Zn 2p in Figure-11, clearly indicating that the oxidation states was +2 in the form of ZnO on the surface [19]. In the survey scan, spectrum Zn, O, Ni, C peaks were characterized (Figure-10). The carbon present in the samples was presumably due to acetate vestige and / or carbon adsorption process present in ambient condition [20, 21].

The splitting of Zn-2p states was about 23 eV, which was induced from the powerful spin-orbit coupling. These numbers were different from the binding energy quantity of stoichiometric ZnO (1045.1 eV for Zn (2p1/2) and 1022.1 eV for Zn (2p3/2)), which can be attributed to the change of charge transfer Zn^{2+} to O^{2-} due to existence of vacancies [22]. By comparing the O-1s curve of all the samples and asymmetric curve was observed in the samples, by fitting these in Gaussian peaks the different types of Oxygen groups in the samples were ranging from 2-4 peaks. The stoichiometric peaks assigned were at 530.50 eV, which was dedicated to O^{2-} ions of Zn-O bonding at crystal lattice [23].

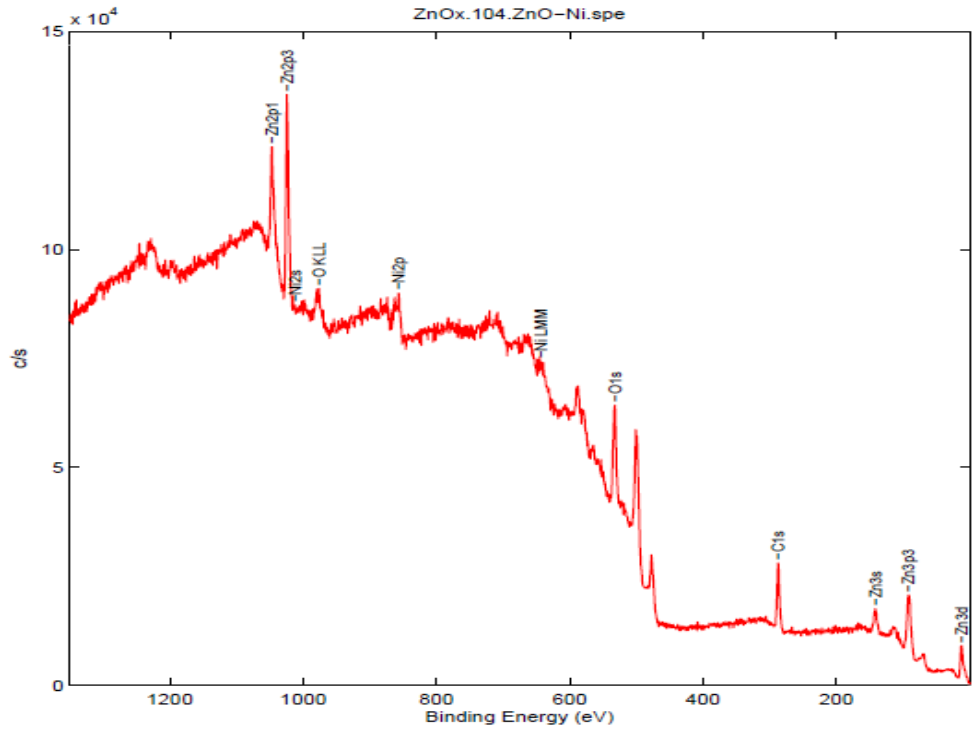

Fig 11: General scan of ZnO-Ni.

The remaining peaks were related to the hydroxyl group adsorption due to structural defects [20] and carbonate species [24, 25].With nickel doping, Os1 peak got deconvulged to one at lower binding energy of 527.08 eV and 532.89 eV which was reported as 1s peak of NiO of Oxygen and 532.89 eV was O in 1s of $Ni(OH)_2$ - NIST database. The peaks of Zn 2p shifts towards higher binding energy with Nickel doping at 854.09 eV, 857.08 eV and 860.78 eV were observed, expressing the formation of defects and thus various energy levels above the valence band.

3.2 Antibacterial activity of nanoparticles

The antibacterial agent is considered as "bactericidal" if it kills bacteria or as "bacteriostatic" if it inhibits their growth. The broth dilution method was used, followed by colony count, through plating serial culture broths dilutions which contained ZnO-NPs and targeted bacteria in agar medium. Gram-positive bacteria have one cytoplasmic membrane with multilayer of peptidoglycan polymer [26], and a thicker cell wall (20-80nm). Whereas, Gram-negative bacteria wall is composed of two cell membrane, an outer membrane and a plasma membrane with a thin layer of peptidoglycan [26] with a thickness of 7-8nm. NPs with size within such ranges can readily pass through the peptidoglycan and hence the cell membranes are highly susceptible to damage. The overall charge of the bacterial cell walls is negative. The ability of NPs to rupture the bacterial cells depends upon the size, shape, surface area, surface defects and surface charge as their surface contains numerous edges and corners, which are potential reactive sites.

The decrease in particle size increases the antibacterial activity has been evaluated [27]. Larger the surface area, better is the anti-bacterial activity [28]. Other factors on which antibacterial activity depends are concentration and crystalline structure of ZnO-NPs [29].

Since ZnO with defects can be active by both UV and visible light, electron-hole pairs ($e^- h^+$) can be created. The hole split H_2O molecules (from the suspension of ZnO) into OH^- and H^+. Dissolved oxygen molecules are transformed to super oxide anions ($*O_2^-$), which in turn react with H^+ to generate (HO_2*) radicals, which upon subsequent collision with electrons produce hydrogen peroxide anions (HO_2^-). They then react with hydrogen ions to produce molecules of H_2O_2. The generated H_2O_2 can penetrate the cell membrane and kill the bacteria [30, 31]. Thus, the formation of reactive oxygen species (ROS):

$ZnO + h\gamma \rightarrow e^- + h^+$
$h^+ + H_2O \rightarrow *OH + H^+$
$e^- + O_2 \rightarrow *O_2^-$
$*O_2^- + H^+ \rightarrow HO_2*$
$HO_2^- + H^+ + e^- \rightarrow H_2O_2$

Since the hydroxyl radicals and super oxides are negatively charged particles, they cannot penetrate into the cell membrane and must remain in direct contact with the outer surface of the bacteria; however H_2O_2 can penetrate into the cell [32]. Thus, the cell membrane ruptures and the lipid flows out killing the cell. The generation of H_2O_2 depends on the surface area of ZnO, which, results in more oxygen species on the surface and the higher antibacterial activity of the smaller NPs. Therefore the bulk ZnO showed less bacterial activity than the NPs. When the particles are small more number can accumulate on the bacteria, killing it faster than the bigger particle. This is the chemical explanation. The other cause may be the physical structure due to which the abrasive surface may rupture the cells leading, it to the fatal damage [33-35].

The enhanced bioactivity of smaller particles is attributed to the higher surface area to volume ratio, resulting in more generation of active oxygen species, killing bacteria more effectively than the bulk. The dominant mechanism is found to be either or both the abrasiveness that is the physical interactions between the NPs and biological cells and the chemical interaction between the hydrogen peroxide and cell membrane. The MIC and MBC of the ZnO-NPs doped with metals of various concentrations on Gram-positive and Gram-negative bacteria have been measured and tabulated (Table-

2). This study can be used as toxicity of metal oxide nanoparticles as biocides and disinfectants. The MIC, MBC and zone of inhibition of the doped samples provide information on the dosage for a particular application along with an antibacterial agent.

Table 2: MIC, MBC of ZnO, ZnO-10V, ZnO-10Ni.

Sample	Bacteria	MIC (µg/ml)	MBC (µg/ml)
ZnO	*E.coli*	400	800
	S.aureus	200	400
ZnO-10V	*E.coli*	400	800
	S.aureus	400	400
ZnO-10Ni	*E.coli*	1600	1600
	S.aureus	800	800

MIC = Minimum Inhibitory Concentration; MBC = Minimum Bactericidal Concentration

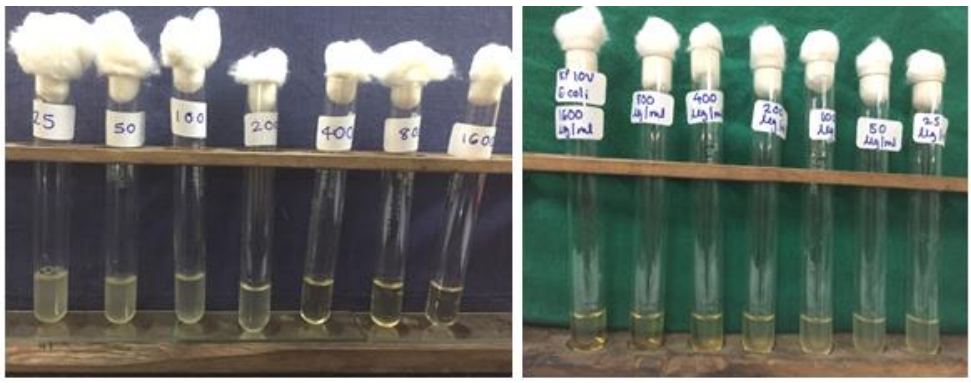

Fig 12: MIC of ZnO with E. coli & S. aureus

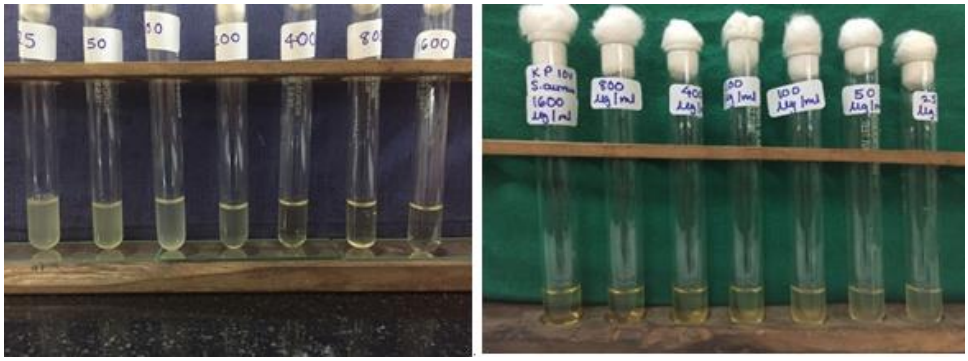

Fig 13: MIC of ZnO-V with E. coli & S. aureus.

Fig-14: MIC of ZnO-Ni with E. coli & S. aureus.

In ZnO-Ni, the incorporation of Ni as an extrinsic impurity into the ZnO matrix, oxygen vacancies were generated which leads to empty oxygen sites. Thus, the interstitial occurrence of zinc and nickel ions will promote the ionic conductivity. This may lead to have either shallow or deep level donors in the band gap of ZnO [36, 37].

4. Conclusion

Antibiotic-resistant bacteria are increasing every year and thus, a new approach using nanoparticles, may be a compelling alternative. The importance and significance of ZnO-NPs, which possess unique properties in the nano range, by improved particle size, concentration, morphology and

surface modification using dopants can emerge as breakthrough in biomedicine, catalysis and food industry. The excellent stability of ZnO-NPs with long shelf-life in comparison with organic-based disinfectants makes it a novel antimicrobial agent. Vanadium as dopant has reduced the band gap resulting in shift in absorption in the visible region. The MIC and MBC were quantified on Gram-positive and Gram-negative bacteria using these particles. Additional research would be required to investigate the exact toxicity mechanism to elucidate the sensitivity of bacteria to ZnO NPs and with dopants.

5. References

1. Fan Z, Lu JG. Zinc oxide nanostructures: synthesis and properties. J Nanosci Nanotechnol. 2005; 5(10):1561-1573.
2. Wang ZL, Song J. Piezoelectric nanogenerators based on zinc oxide nanowire arrays. Science. 2006; 312(5771): 242-246.
3. Janotti A, Van de Walle CG. Fundamentals of zinc oxide as a semiconductor. Rep Prog Phys. 2009; 72(12): 126501.
4. Wang ZL. Zinc oxide nanostructures: growth, properties and applications. J. Phys.: Condens Matter. 2004; 16(25):R829-R858.
5. Zhang Y, Ram MK, Stefanakos EK, Goswami DY. Synthesis, characterization, and applications of ZnO nanowires. J. Nanomater. 2012; 2012:1-22.
6. Schmidt-Mende L, MacManus-Driscoll JL. ZnO-nanostructures, defects, and devices. Mater Today. 2007; 10(5):40-48.
7. Wellings J, Chaure N, Heavens S, Dharmadasa I. Growth and characterisation of electrodeposited ZnO thin films. Thin Solid Films. 2008; 516(12):3893-3898.
8. Song Z, Kelf TA, Sanchez WH, Roberts MS, Rička J, Frenz M, *et al*. Characterization of optical properties of ZnO nanoparticles for quantitative imaging of transdermal transport. Biomed. Opt. Express. 2011; 2(12):3321-3333.
9. Mishra Y, Chakravadhanula V, Hrkac V, Jebril S, Agarwal D, Mohapatra S *et al*. Crystal growth behaviour in Au–ZnO nanocomposite under different annealing environments and photoswitchability. J Appl Phys. 2012; 112(6):064308.
10. Seil JT, Webster TJ. Antimicrobial applications of nanotechnology: methods and literature. Int J Nanomed. 2012; 7: 2767-2781.
11. Colon G, Ward BC, Webster TJ. Increased osteoblast and decreased Staphylococcus epidermidis functions on nanophase ZnO and TiO2. J. Biomed Mater Res. 2006; 78(3):595-604.
12. Padmavathy N, Vijayaraghavan R. Enhanced bioactivity of ZnO nanoparticles - An antimicrobial study. Sci Technol Adv Mater. 2008; 9(3):035004.
13. Pearton SJ, Abernathy CR, Overberg ME, Thaler GT, Norton DP, Theodoropoulou N, *et al*. Wide band gap ferromagnetic semiconductors and oxide. J Appl Phys. 2003; 93(1):1-13.
14. Ahmed F, Arshi N, Anwar MS, Lee SH, Byon ES, Lyu NJ, Koo BH. Effect of Ni substitution on structural, morphological and magnetic properties of Zn1-xNixO nanorods. Curr Appl Phys. 2012; 12(Suppl 2):S174-S177.
15. Konstantinou IK, Albanis TA. TiO2-assisted photocatalytic degradation of azo dyes in aqueous solution: kinetic and mechanistic investigations: A review. Applied Catalysis B: Environmental. 2004; 49(1):1-14.
16. Xu C, Cao L, Su G, Liu W, Qu X, Yu Y. Preparation, characterization and photocatalytic activity of Co-doped ZnO powders. J Alloy Comp. 2010; 497(1-2):373-376.
17. Ana Stanković LV, Marković S, Dimitrijević S, Škapin SD, Uskoković D. Morphology Controlled hydrothermal synthesis of ZnO particles and examination of their antibacterial properties on *Escherichia coli* and *Staphylococcus aureus* bacterial cultures. Tenth Young Researchers' Conference, Materials Science and Engineering, Belgrade, Serbia, 2011, 62.
18. Berry V, Gole A, Kundu S, Murphy CJ, Saraf RF. Deposition of CTAB-terminated nanorods on bacteria to form highly conducting hybrid systems. J Am Chem Soc. 2005; 127(50):17600-17601.
19. Myung Y, Jang DM, Sung TK, Sohn YJ, Jung GB, Cho YJ, *et al*. Composition-Tuned ZnO−CdSSe Core−Shell Nanowire Arrays. ACS Nano. 2010; 4(7):3789-3800.
20. Al-Gaashani R, Radiman S, Daud AR, Tabet N, Al-Douri Y. XPS and optical studies of different morphologies of ZnO nanostructures prepared by microwave methods. Ceramics International. 2013; 39(3):2283-2292.
21. Wahab R, Ansari S, Kim Y, Seo H, Kim G, Khang G, *et al*. Low temperature solution synthesis and characterization of ZnO nano-flowers. Mater Res Bull. 2007; 42(9):1640-1648.
22. Sahu RK, Ganguly K, Mishra T, Mishra M, Ningthoujam RS, Roy SK, *et al*. Stabilization of intrinsic defects at high temperatures in ZnO nanoparticles by Ag modification. J Colloid Interface Sci. 2012; 366(1):8-15.
23. Zheng JH, Song JL, Li XJ, Jiang Q, Lian JS. Experimental and first-principle investigation of Cu-doped ZnO ferromagnetic powders. 2011; 46(11):1143-1148.
24. Chong MN, Jin B, Chow CWK, Saint C. Recent developments in photocatalytic water treatment technology: A review. Water Res. 2010; 44(10):2997-3027.
25. Ng J, Xu S, Zhang X, Yang HY, Sun DD. Hybridized Nanowires and Cubes: A Novel Architecture of a Heterojunctioned TiO2/SrTiO3 Thin Film for Efficient Water Splitting. Adv Functional Mater. 2010; 20(24):4287-4294.
26. Fu G, Vary PS, Lin CT. Anatase TiO2 nanocomposites for antimicrobial coatings. J Phys Chem B. 2005; 109(18):8889-8898.
27. Raghupathi KR, Koodali RT, Manna AC. Size-dependent bacterial growth inhibition and mechanism of antibacterial activity of zinc oxide nanoparticles. Langmuir. 2011; 27(7):4020-4028.
28. Yamamoto O. Influence of particle size on the antibacterial activity of zinc oxide. Int. J Inorg Mater. 2001; 3(7):643-646.
29. Jeng HA, Swanson J. Toxicity of metal oxide nanoparticles in mammalian cells. J Environ Sci Health A. 2006; 41(12):2699-2711.
30. Tokumoto M, Briois V, Santilli CV, Pulcinelli SH. Preparation of ZnO Nanoparticles: Structural Study of the Molecular Precursor. J Sol-Gel Sci Technol. 2003; 26(1-3):547-551.
31. Du YL, Zhang MS, Hong J, Shen Y, Chen Q, Yin Z. Structural and optical properties of nanophase zinc oxide. Appl Phys A. 2003; 76:171-176.
32. Padmavathy N, Vijayaraghavan R. Enhanced bioactivity

of ZnO nanoparticles - An antimicrobial study. Sci Technol Adv Mater. 2008; 9(3):035004.
33. Rana S, Rawat J, Sorensson MM, Mishra RDK. Antimicrobial function of Nd3+-doped anatase titania-coated nickel ferrite composite nanoparticles: A biomaterial system. Acta Biomater. 2006; 2(4):421-432.
34. Emami-Karvani Z, Chehrazi P. Antibacterial activity of ZnO nanoparticle on gram-positive and gram-negative bacteria. Afr J Microbiol Res. 2011; 5(12):1368-1373.
35. Wang LW, Xu Z, Meng LJ, Teixeira V, Song SG, Xu XR. Influence of Concentration of Vanadium in Zinc Oxide on Structural and Optical Properties with Lower Concentration. Chin Phys Lett. 2009; 26(7):077801.
36. Chandrasekaran A, Prasankumar T, Jose S, Kandasamy A, Ekstrum C, Pearce J, *et al*. Synthetic Method Dependent Physicochemical Properties and Electrochemical Performance of Ni-Doped ZnO. Chemistry Select. 2017; 2(28):9014-9023.
37. Sirelkhatim A, Mahmud S, Seeni A, Kaus NHM, Ann LC, Bakhori SKM, *et al*. Review on Zinc Oxide Nanoparticles: Antibacterial Activity and Toxicity Mechanism. Nano-Micro Lett. 2015; 7(3):219-242.